

**Supporting Information for:**

**Wormlike Micelles of a Cationic Surfactant in Polar Organic Solvents: Extending Surfactant Self-Assembly to New Systems and Sub-Zero Temperatures**

Niti R. Agrawal<sup>1</sup>, Xiu Yue<sup>1,2</sup>, Yujun Feng<sup>3\*</sup> and Srinivasa R. Raghavan<sup>1\*</sup>

<sup>1</sup>Department of Chemical & Biomolecular Engineering, University of Maryland, College Park, Maryland 20742, USA

<sup>2</sup>Xinjiang Technical Institute of Physics & Chemistry, Chinese Academy of Sciences, Urumqi 830011, China

<sup>3</sup>Polymer Research Institute, State Key Lab of Polymer Materials Engineering, Sichuan University, Chengdu 610065, China

\*Corresponding authors. Email: [sraghava@umd.edu](mailto:sraghava@umd.edu), [yjfeng@scu.edu.cn](mailto:yjfeng@scu.edu.cn)

- Fig S1: Vial photos showing coacervation of EHAC/NaTos samples in glycerol.
- Fig S2: Viscosity data in formamide at various temperatures.
- Fig S3: Freezing points of mixtures containing glycerol (Gly).
- Fig S4: Experiment demonstrating the utility of viscoelastic WLMs in Gly-EG mixtures.
- Fig S5: Model fits to SANS data shown in the paper.
- Fig S6: IFT analysis of SANS data shown in the paper.

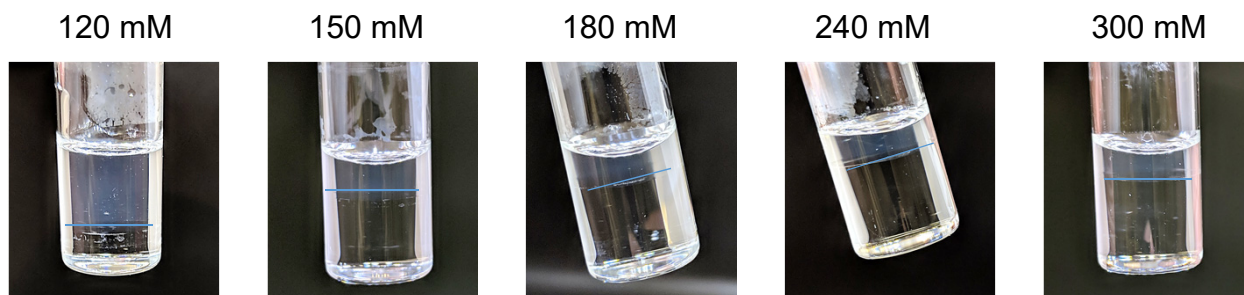


**Figure S1. Vial photos showing coacervation of EHAC/NaTos samples in glycerol.** Samples of EHAC/NaTos in glycerol show a 2-phase region, as discussed in Figure 3 of the main paper. Photos of selected samples are shown here. The samples contain 60 mM EHAC and varying NaTos (120, 150, 180, 240 and 300 mM). All samples show two co-existing liquid phases, i.e., coacervation. The phase boundary between the surfactant-rich phase (bluish) and the salt-rich phase (colorless) is indicated in each sample by a line for clarity.

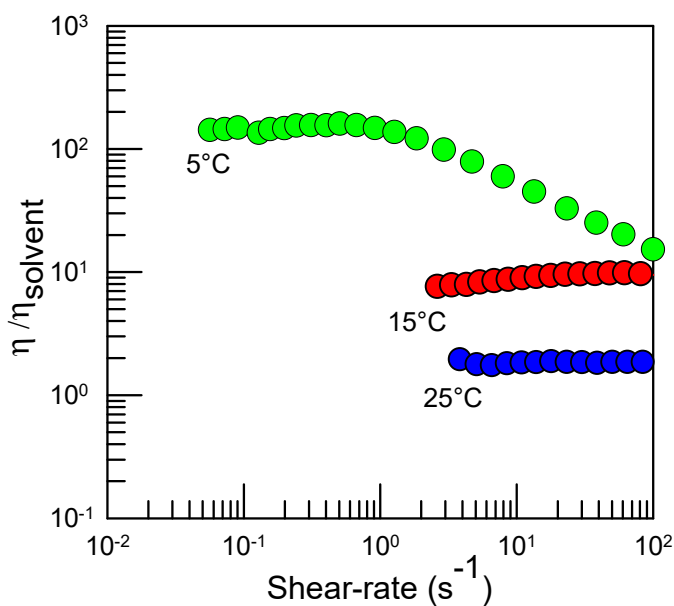


**Figure S2. Viscosity data in formamide at different temperatures.** The relative viscosity data for a sample of 60mM EHAC + 90 mM NaSal in formamide is shown at different temperatures of 25, 15 and 5°C. The data at 5°C alone is plotted in Figure 6 of the main paper. Note that the sample remains Newtonian at 15 and 25°C while it is shear-thinning at 5°C.

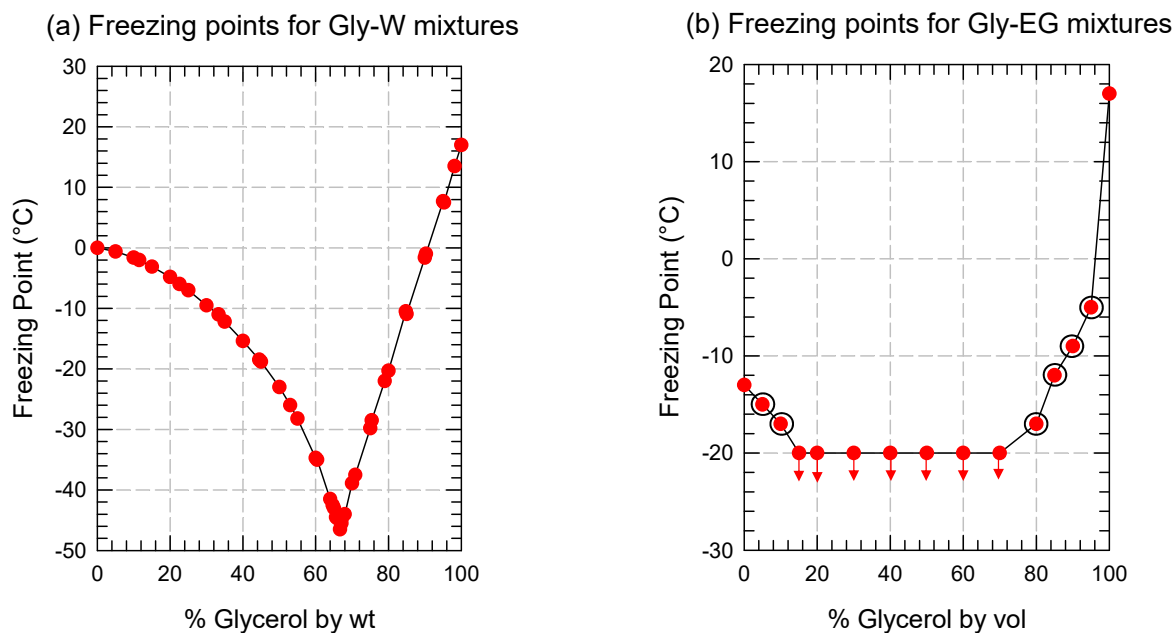


**Figure S3. Freezing points of mixtures containing glycerol (Gly).** The freezing points of glycerol-water (Gly-W) mixtures (a) and glycerol-ethylene glycol (Gly-EG) mixtures (b) are shown here. Gly-water data are replotted from Ref. 38. For Gly-EG mixtures, the samples were observed at  $-20^{\circ}\text{C}$  (freezer) and  $-5^{\circ}\text{C}$  (circulating bath), and the phase (solid or liquid) was estimated from the flowability of the sample. The red arrows indicate a freezing point below  $-20^{\circ}\text{C}$ , i.e., the sample remained liquid under these conditions. The points with black circles are interpolated values for the freezing points between  $-5$  and  $-20^{\circ}\text{C}$ .

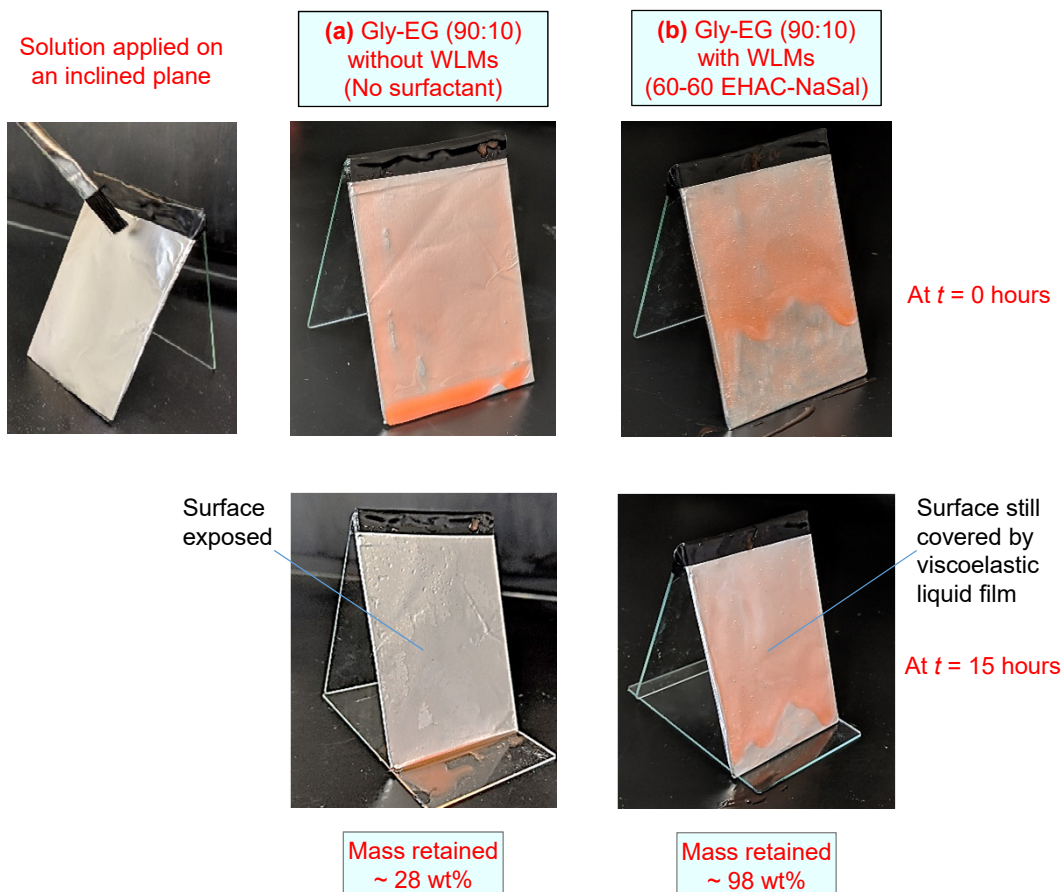


**Figure S4. Experiment demonstrating the utility of viscoelastic WLMs in Gly-EG mixtures.** A Gly-EG (90:10 v/v) mixture has a freezing point below  $-20^{\circ}\text{C}$ . It can be rendered viscoelastic (due to the formation of WLMs) by adding EHAC-NaSal (60-60 mM). The bare solvent mixture and its viscoelastic counterpart are compared in a simple visual test. For this, inclined aluminum surfaces were created using glass slides covered with aluminum foil. Red iron oxide pigment (0.1 wt%) was added to the solutions for better visualization. Approximately 1 g of the respective samples were applied onto the surfaces using a paint brush (left top) at time  $t = 0$ , and the surfaces were then placed in the freezer ( $T \sim -20^{\circ}\text{C}$ ) for 15 hours. Due to the low freezing point of the solvent, neither sample froze into a solid. Results are shown in (a) for the Gly-EG solvent mixture and in (b) for the viscoelastic sample of WLMs in Gly-EG. In (a), the liquid initially coats the surface (top), but it quickly flows down the surface and collects in a pool below (bottom). The surface is thereby left exposed. Only 28% of the liquid mass was measured to remain on the surface. In (b), the viscoelastic sample coats the surface as a thin film (top), and this film persists even after 15 hours (bottom). 98% of the sample mass was found to remain on the surface.

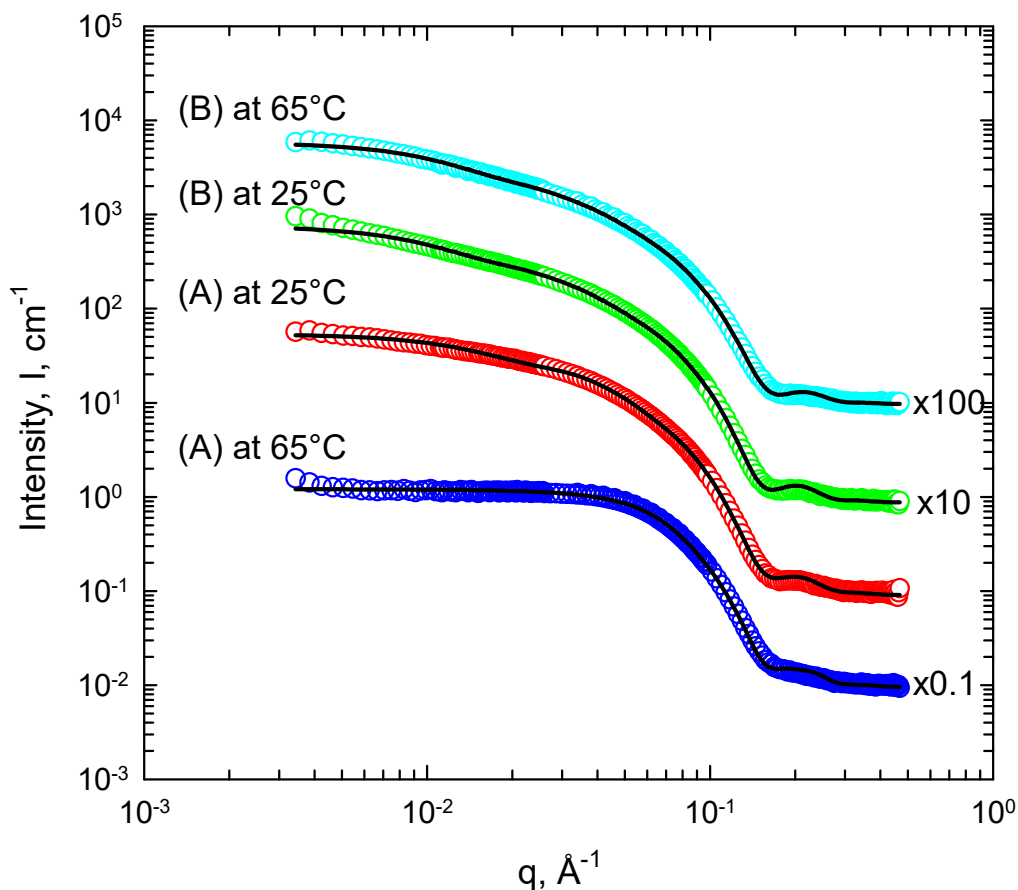


**Figure S5. Model fits to SANS data shown in the paper.** Plots of scattered intensity  $I$  vs. wave-vector  $q$  are shown for sample A (EHAC-NaSal 60-30 mM) and sample B (EHAC-NaSal 60-60 mM) at two different temperatures: 25 and 65°C. In each case, the data (open circles) are fit to a model, and the model fits are shown as continuous lines. The model is discussed below on page S-7. Parameters corresponding to the fits are shown in the table below.

**Table S1. Fitting parameters for the data in Figure S5.**

The selected model is for cylinders having a polydisperse radius and interacting via hard-sphere interactions.

Sample EHAC-NaSal (mM)	Temp (°C)	Radius (Å)	Distribution of Radius	Length (Å)	Volume Fraction	Reduced $\chi^2$
60-30	25	23.9	0.105	336	0.057	35.8
	65	23.5	0.088	93	0.076	33.5
60-60	25	24.0	0.096	473	0.036	33.2
	65	22.7	0.102	425	0.028	27.1

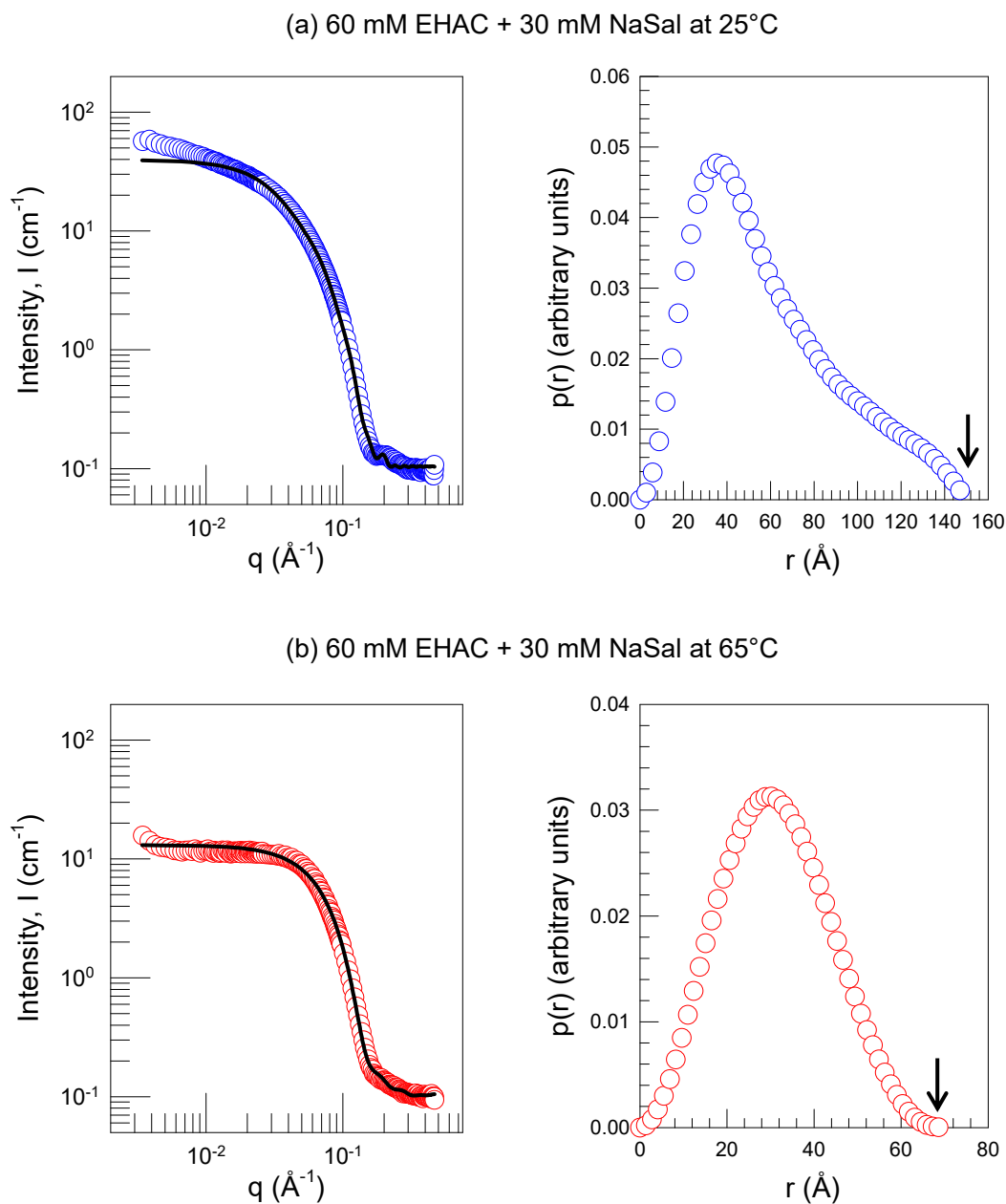


**Figure S6. IFT analysis of SANS data shown in the paper.** The SANS data for the sample of EHAC-NaSal (60-30 mM) in glycerol at 25°C and 65°C are analyzed by the IFT method (see page S-7 below) to obtain the corresponding pair distance distribution functions  $p(r)$ . (a) At 25°C, the  $p(r)$  plot is asymmetrical and indicative of elongated micelles (WLMs). The point where  $p(r)$  hits the x-axis ( $\sim 150$  Å), indicated by the arrow, is an estimate for the micellar length. (b) At 65°C, on the other hand,  $p(r)$  is symmetrical, which is indicative of spherical micelles. The point where  $p(r)$  hits the x-axis ( $\sim 70$  Å), indicated by the arrow, is an estimate for the micellar diameter.

**SANS Modeling (Figure S5):** SANS data in the figure were fit using a model available in the SasView software package provided by NIST. This model is described by equations S1 to S6. It models the structures in the sample as cylinders interacting via hard-sphere interactions. The cylinders are modeled as being polydisperse in their radius, but monodisperse in their length. Fitting parameters from the model fits are provided in Table S1.

The form factor  $P(q)$  in the model accounts for the size and shape of the scatterers. For cylinders of radius  $r$  and length  $L$ , it is given by the following (see Refs. 45, 46 in the main paper):

$$P(q) = \frac{\text{scale}}{V_{\text{cyl}}} \int_0^{\pi/2} F^2(q, \alpha) \sin \alpha \, d\alpha \quad (\text{S1})$$

where the scattering amplitude  $F$  is given by:

$$F(q, \alpha) = 2V_{\text{cyl}} (\rho_{\text{cyl}} - \rho_{\text{solv}}) j_0\left(\frac{qL}{2} \cos \alpha\right) \left[ \frac{J_1(qr \sin \alpha)}{qr \sin \alpha} \right] \quad (\text{S2})$$

Here, ‘scale’ is the volume fraction of cylinders,  $V_{\text{cyl}} = \pi r^2 L$  is the volume of each cylinder,  $j_0(x) = \sin(x)/x$ ,  $J_1$  is the first-order Bessel function, and  $\alpha$  is the angle between the cylinder axis and the scattering vector  $q$ .  $\rho_{\text{cyl}}$  and  $\rho_{\text{solv}}$  are the scattering length densities of the cylinder and the solvent. To account for polydispersity in the radius,  $P(q)$  is averaged over a Schulz distribution of the cylinder radius. The size-averaged  $P(q)$  is given by the following, where  $f(r)$  is the normalized Schulz distribution of the radius  $r$  and  $V_{\text{poly}}$  is the volume of the polydisperse object.

$$\bar{P}(q) = \frac{1}{V_{\text{poly}}} \int_0^{\infty} P(q) f(r) dr \quad (\text{S3})$$

Next, the structure factor  $S(q)$  accounts for interactions between the cylinders:

$$S(q) = 1 + 4\pi n_p \int_0^{\infty} [g(r) - 1] \frac{\sin qr}{qr} r^2 dr \quad (\text{S4})$$

Here  $g(r)$  represents the pair correlation function and  $n_p$  is the number of particles (scatterers) per unit volume. Various models for  $S(q)$  are available in SasView. We have used the simplest one, which assumes that the particles are ‘hard spheres’, i.e., that they have no interaction at long distances and an infinite repulsion upon contact (see Ref. 45).

**SANS Analysis by IFT (Figure S6):** SANS data in the figure were analysed by the IFT approach through the SasView software package provided by NIST. In IFT, a Fourier transformation of the scattering intensity  $I(q)$  is performed to obtain the pair distance distribution function  $p(r)$  in real space (with  $r$  being distance in real space).  $p(r)$  provides structural information about the scatterers, such as their shape and maximum dimension. The relationship between  $I(q)$  and  $p(r)$  is given by the following equation (see Ref. 47):

$$I(q) = 4\pi \int_0^{\infty} p(r) \frac{\sin(qr)}{qr} dr \quad (\text{S5})$$

The characteristic forms of  $p(r)$  for structures such as spherical and cylindrical micelles has been discussed in previous papers (see Ref. 48, for example).